JOURNAL OF APPLIED POLYMER SCIENCE VOL. VI, ISSUE NO. 21, PAGES 352-360 (1962)

A Comparison of the Static and Dynamic Strengths of Several Phenolic- and Epoxy-Impregnated Paper and Cloth Honeycombs in Compression

R. M. LACEY and J. E. SMITH

Sandia Corporation, Albuquerque, New Mexico

The advent of the missile age accompanied by the more stringent requirements of space vehicles over conventional types of aircraft has renewed interest in structural members of optimum strength-to-weight and rigidity-to-weight ratios, and has given further impetus to the continuing search for rigid high-strength low-weight structures. Prominent among the more successful materials—as evidenced by their increasing use in missiles, high-performance aircraft, and other applications where lightness, strength, and rigidity are at a premium—have been the various organic resin-impregnated paper and cloth honeycomb sandwich structures, especially in those applications where low thermal conductivity is also important. Joseph[1] reports a rigidity factor (EI) of 792,000 for 1-in. thick paper honeycomb panel faced with 0.016-in. aluminum which weighs only 0.75 lb./sq. ft., or $^1/_{16}$ the weight of steel, $^1/_{10}$ the weight of aluminum, and $^1/_5$ the weight of birch plywood, of the same rigidity and thickness. The widespread interest in these new materials has prompted extensive investigation of the mechanical properties of the various resin-impregnated paper and cloth honeycomb systems. As a result, materials properties data, methods of manufacture, and methods of design with the honeycomb sandwich are widely reported in the literature.[2-4]

Since these materials are often used as compression members and are typically brittle, the compressive strength, i.e., the stress that the material is capable of sustaining without catastrophic failure, has been of particular interest. Since the intended application of these honeycomb materials quite often entails dynamic loading, it became apparent in early studies that high-speed compression data were desirable. However, because of the relative complexity of controlled high rate of loading devices and the difficulty of analyzing results obtained from simple dynamic tests, the availability of dynamic stress–strain data has lagged considerably behind the more readily obtained slow-speed or "static" data. Consequently, structural members intended to sustain shock loadings have quite often been designed with static data, and a reliance largely on proof-testing for guarantee of structural integrity.

In the present study, an attempt was made to determine the dynamic compression behavior of these materials and to compare this with static behavior. Five selected organic honeycomb materials, two with woven cotton cloth base and three with Kraft paper base, were tested in uniaxial compression at room temperature. Static tests were conducted in a hydraulic testing machine with the strain rate controlled at 1%/min. throughout the test. Dynamic tests were conducted with a high-pressure gas-operated machine which produced strain rates up to 650/min. but did not provide constant strain rate throughout the test. Both static and dynamic strengths were found to vary directly with the apparent density of the sample. Dynamic strengths were greater than static for these materials, and dynamic elongation less than

TABLE I
Sample Designations and Descriptions

Sample designation	Description
PVB	$^3/_8$-in. cell size, 80-lb. Kraft paper, Bakelite BLS-2700 phenolic- and polyvinyl butyral-impregnated
MDA	$^3/_8$-in. cell size, 80-lb. Kraft paper, Epon 828 epoxy- and methane diamine-impregnated
1100	$^3/_8$-in. cell size, 80-lb. Kraft paper, Bakelite BRL-1100 phenolic-impregnated
C-1/4	$^1/_4$-in. cell size, cotton cloth honeycomb, Bakelite BLS-2700 phenolic-impregnated
C-7/16	$^7/_{16}$-in. cell size, cotton cloth honeycomb, Bakelite BLS-2700 phenolic-impregnated

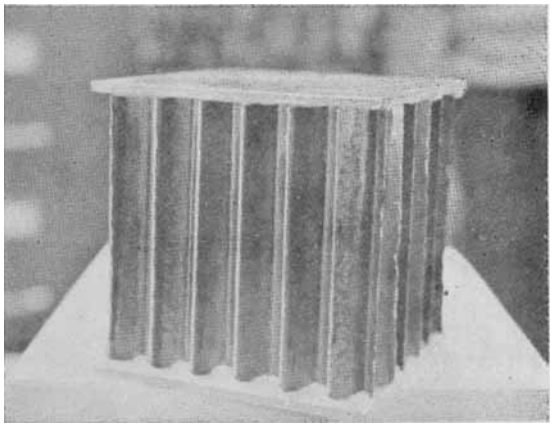

Fig. 1. Compression sample.

static, such that the energies of fracture were less in the dynamic tests than in the static tests.

SAMPLES

The sample designations and descriptions are shown in Table I.

In all cases the material was cut into 2-in. cube samples (Fig. 1) and loaded in the direction of the longitudinal axis of the cell. A $^1/_{16}$-in. aluminum sheet was cemented to either end of the sample with Furane Plastics Epibond 104, to provide a contacting surface for the compression platens. The apparent density of each sample was determined before this cementing procedure by dividing the weight of the sample by the volume of the smallest rectangular parallelepiped which would contain the sample.

TEST PROCEDURE

Static Compression Tests

Static compression tests were run on a 10,000-lb. Baldwin Mark G testing machine with a constant crosshead speed of 0.020 in./min. Autographic records of compression force versus specimen deflection were obtained from the machine recorder driven by SR-4 strain-gauge load cells and an LVDT-type compressive deflectometer.

Dynamic Compression Tests

To obtain dynamic stress versus strain curves, a Convair 6-in. dynamic stressing facility was used. This machine uses the controlled rapid application of high-pressure gas to a piston, providing a trapezoidal force application program. The samples were placed on the anvil, and the load column allowed to rest on the top of the sample, as

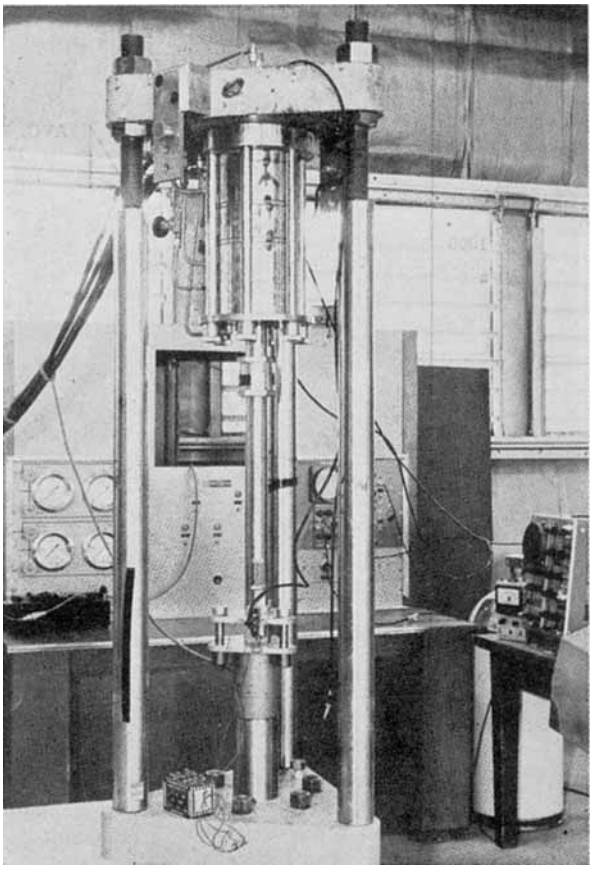

Fig. 2. Dynamic stressing facility.

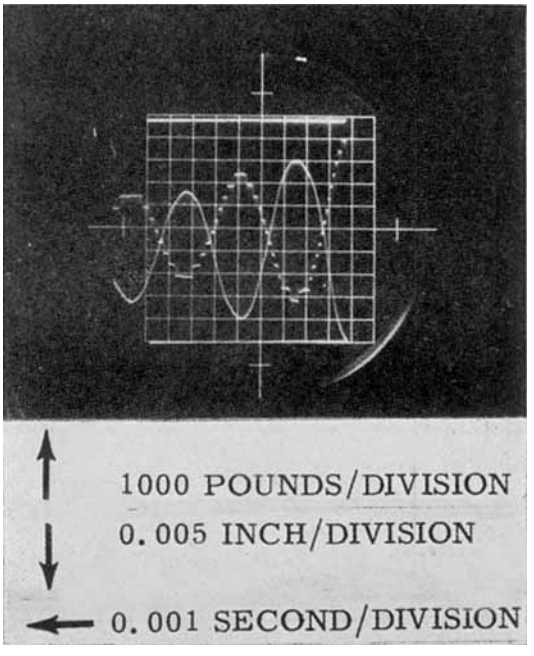

Fig. 3. Typical force versus time and deflection versus time record: lower horizontal line, zero load; upper horizontal line, zero deflection.

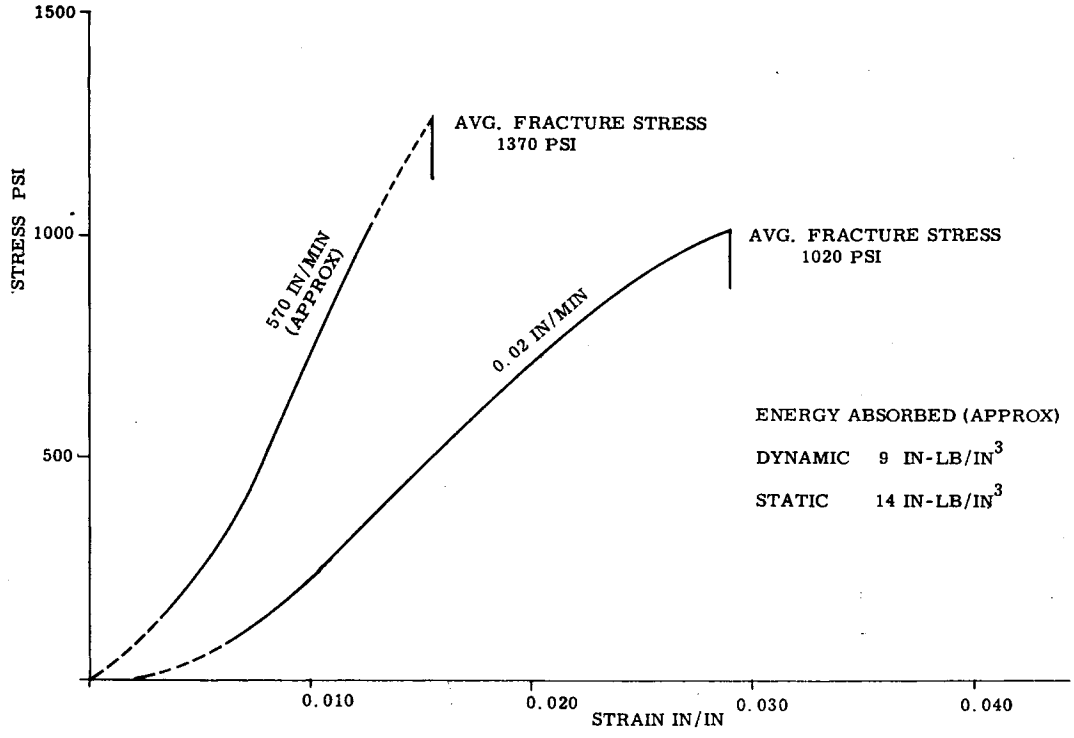

Fig. 4. Average static and dynamic stress versus strain, composition PVB, average density 5.8 lb./cu. ft.

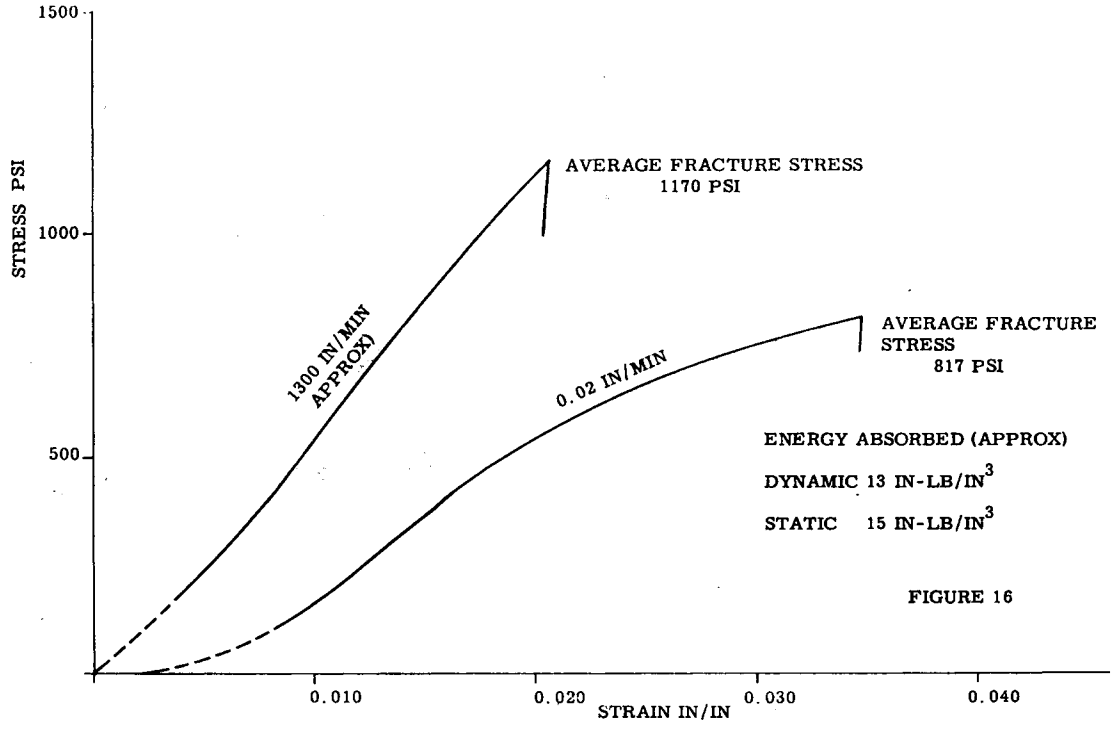

Fig. 5. Average static and dynamic stress versus strain, composition MDA, average density 5.7 lb./cu. ft.

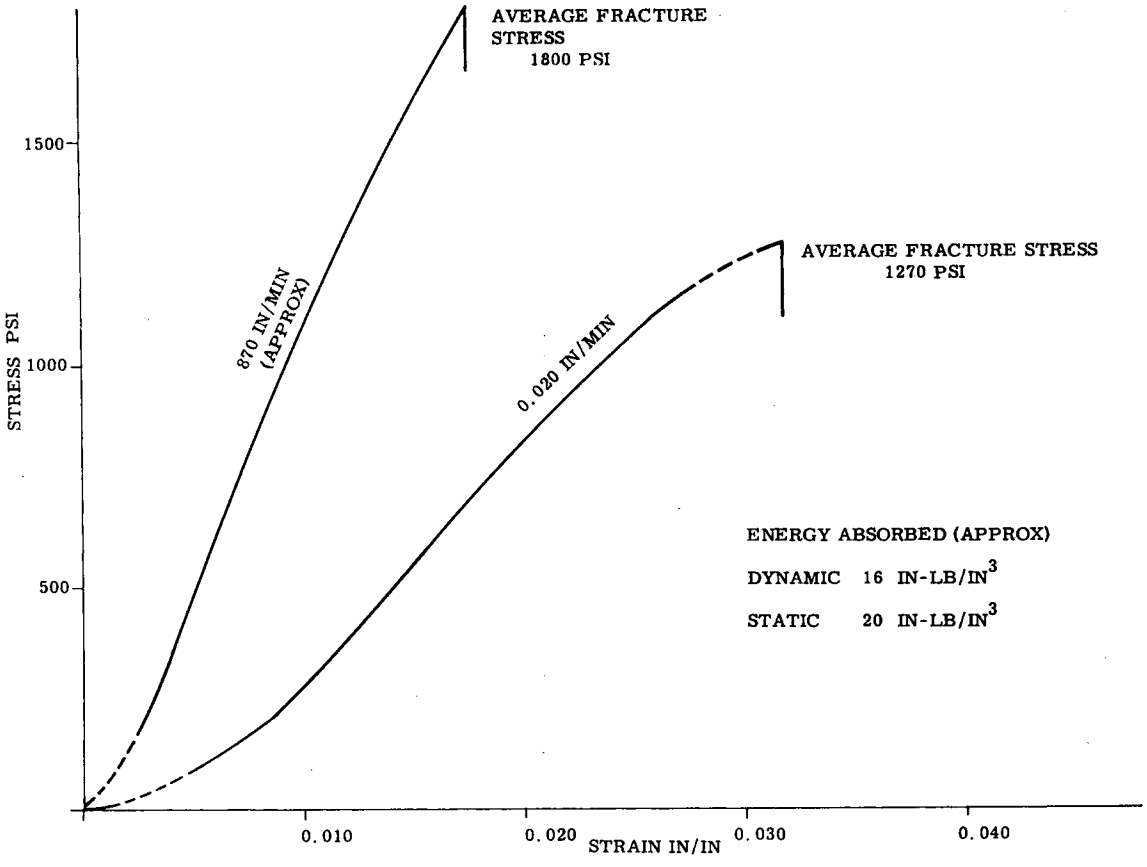

Fig. 6. Average static and dynamic stress versus strain, composition 1100, average density 7.15 lb./cu. ft.

shown in Figure 2. The weight of the load column and consequent preload on the sample is approximately 35 lb., or 9 psi. The equipment is instrumented to display compressive force versus time and sample deflection versus time on a single oscilloscope by means of a chopping technique. A Polaroid photograph of this display (Fig. 3) was used to plot stress versus strain.

During these dynamic tests an attempt was made to load the samples to a point just below fracture, to avoid damage to the compressometer. The average fracture stress, shown in Figures 4 through 8, was determined separately. Both unused samples and samples that had previously been loaded to a point just below fracture were used in this determination.

The strain rates varied considerably in these dynamic tests, since the machine does not control strain rate but rather the force applied to the piston. This force is controlled to increase at a constant rate to a fixed peak value which is then held constant. The resulting force applied to the specimen consists of this form with the addition of sinusoidal oscillations at the natural frequency of the specimen, piston, and load shaft system. The actual strain rate varies in a similar manner, and must be determined experimentally for each type of specimen. The average deformation rates for the samples tested varied from 570 to 1300 in./min.

Measurement of Dynamic Force

A relatively stiff (7.5×10^6 lb./in.) load cell is placed directly beneath the sample. The output of an SR-4 strain-gauge bridge mounted on this load cell is applied to one of the vertical inputs of the oscilloscope, causing a beam deflection proportional to the force transmitted to the cell by the sample. Since the load cell is stiff compared with the sample, the resonant frequency of the moving mass–load cell system is high in comparison with the moving mass–specimen system, indicating that spurious load signals caused by load cell resonance should not be observed at the loading rates used in this study. This is seen to be the case in Figure 3, in which the ringing occurred at the

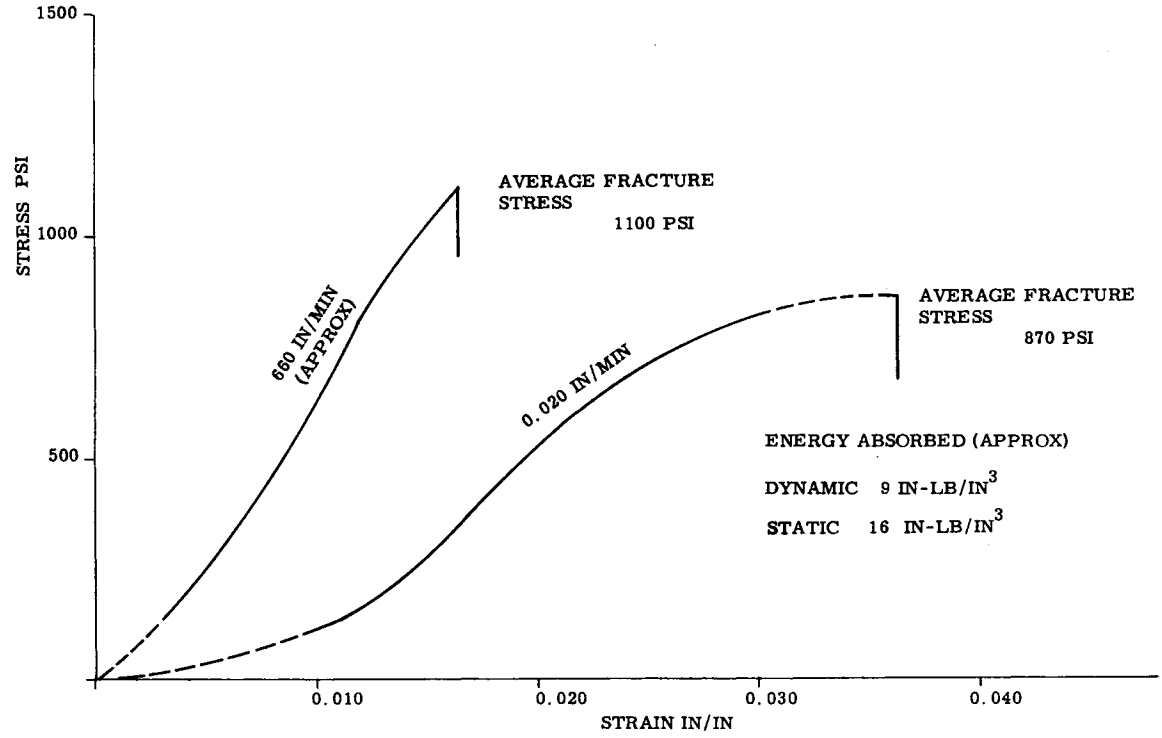

Fig. 7. Average static and dynamic stress versus strain, composition C-1/4, average density 7.05 lb./cu. ft.

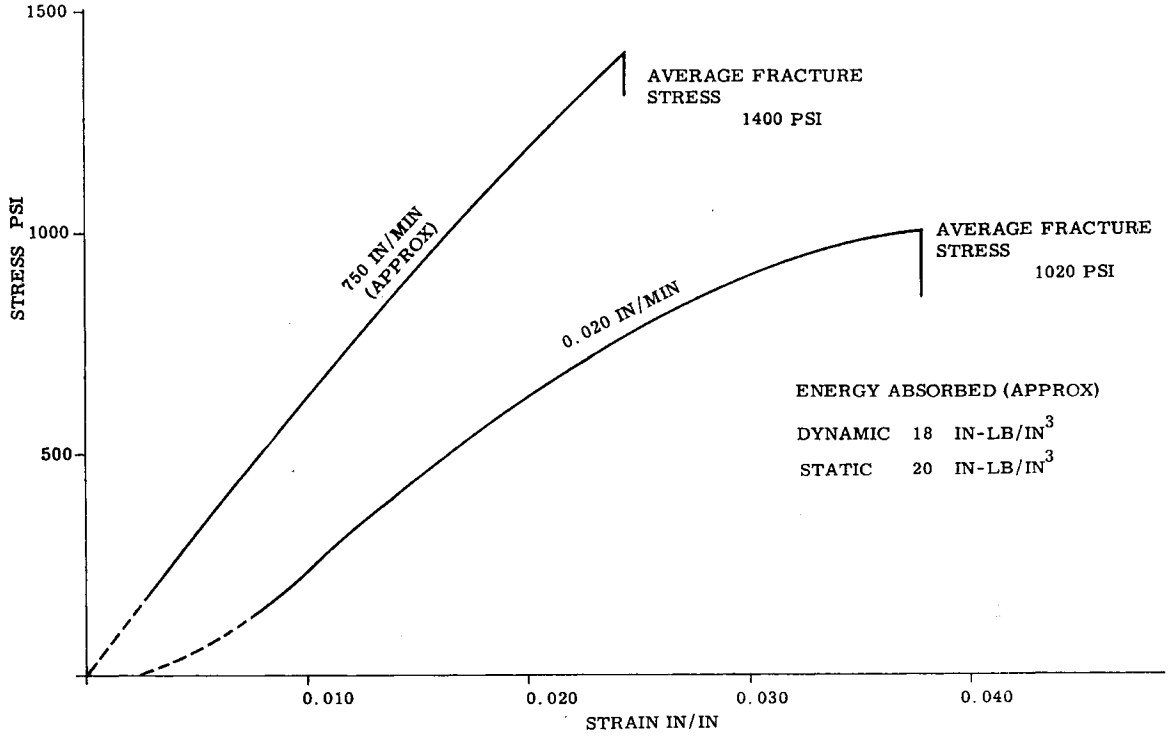

Fig. 8. Average static and dynamic stress versus strain, composition C-7/16, average density 8.25 lb./cu. ft.

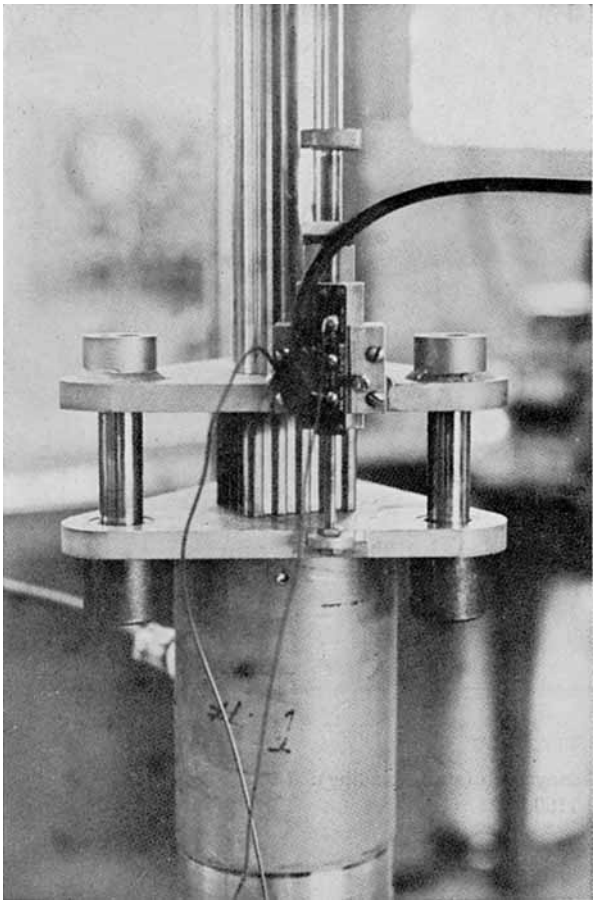

Fig. 9. Deflection measuring device.

predicted resonant frequency of the mass-specimen system (200 cycles/sec.) and in which no evidence of ringing at the mass–load cell frequency (1500 cycles/sec.) is seen.

Measurement of Deflection

To determine the amount of sample deflection, the sample is compressed between two parallel platens (Fig. 9). Parallelism is maintained by the use of three guide rods moving through hardened steel bushings. A linear potentiometer deflection gauge with battery voltage supply is rigidly attached to the upper platen. The sliding contact is secured to the lower platen so that the output voltage varies linearly as the distance between the platens changes. The output of the deflection gauge is applied to the second vertical input of the oscilloscope, causing a beam deflection proportional to the relative motion of the platens. Discontinuities seen in deflection records (Fig. 3) are caused by the discrete stepping of the deflection gauge signal as the wiper alternately makes and breaks electric contact with the potentiometer windings. Analysis of these records is accomplished by smoothing a curve through the mid-points of these steps, which in effect refers each voltage step to the physical center of its particular winding.

RESULTS

To compare the static and dynamic behavior of the various materials, average stress–strain curves were computed for each material from the static and dynamic data recorded (Figs. 5–9). The concave upward initial portion of these curves is not completely established as a material property, and may be due to the method of loading or the use of aluminum end plates on the samples. In any case, this uncertainty is limited to the small initial portion of the curves. Since the apparent density varied from sample to sample of the same material, these curves are considered typical of the average density material as indicated on each figure. This technique is justified by the very similar behavior of the various samples, and by the good correlation of fracture strengths with apparent sample density, as shown in Figures 10–12. In addition, this method of presentation gives results which are applicable to larger volumes of material wherein a certain amount of mechanical averaging of behavior is expected as a result of local variations of apparent density.

DISCUSSION AND CONCLUSIONS

As shown in Figures 4 through 8, the honeycomb materials responded differently to rapid loading than to the much slower static loading. Generally they sustained 30–40% higher stress before failure when loaded at the higher rate. At the same stress level, the dynamically loaded specimens exhibited approximately one half the strain of those loaded slowly. It should be specifically noted that the trend of these five materials to higher fracture strengths and lower elongations with increased loading rate is not established as a general trend except for very similar materials performing under the same conditions. Also, the designer is not necessarily "safe" in using static stress–strain data for these materials in the design of structural components intended to sustain shock loading. Despite the fact that the five materials tested are capable of withstanding higher stresses before fracture under rapid loading than when loaded slowly, an examination of the curves (Figures 4 through 8) reveals that in each case prior to fracture

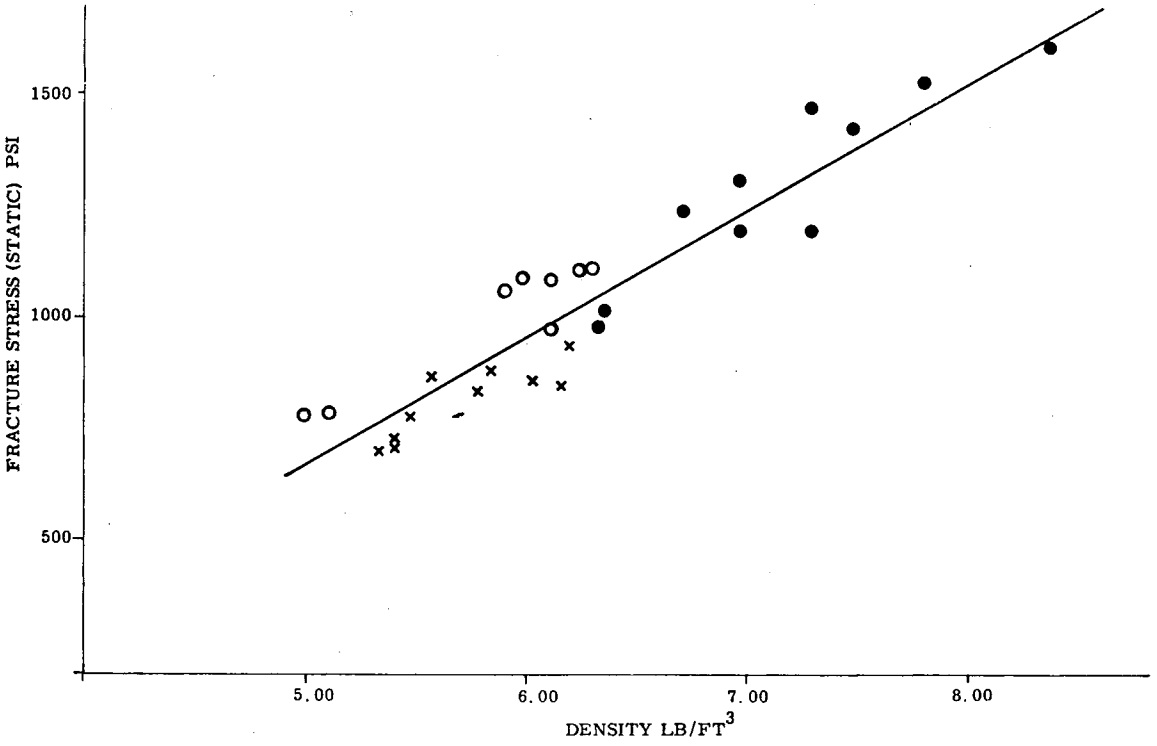

Fig. 10. Fracture stress versus density for paper honeycomb (static loading): (O) PVB; (×) MDA; (●) 1100.

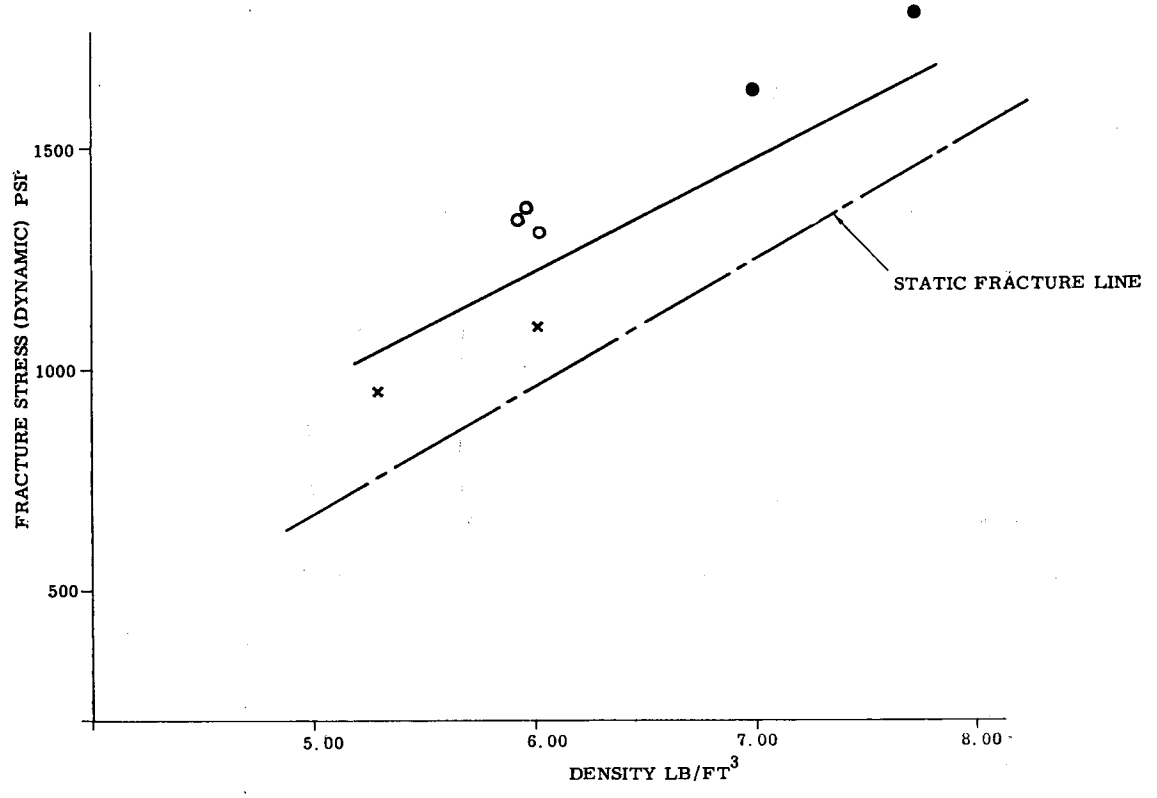

Fig. 11. Fracture stress versus density for paper honeycomb (dynamic loading): (O) PBV; (×) MDA; (●) 1100.

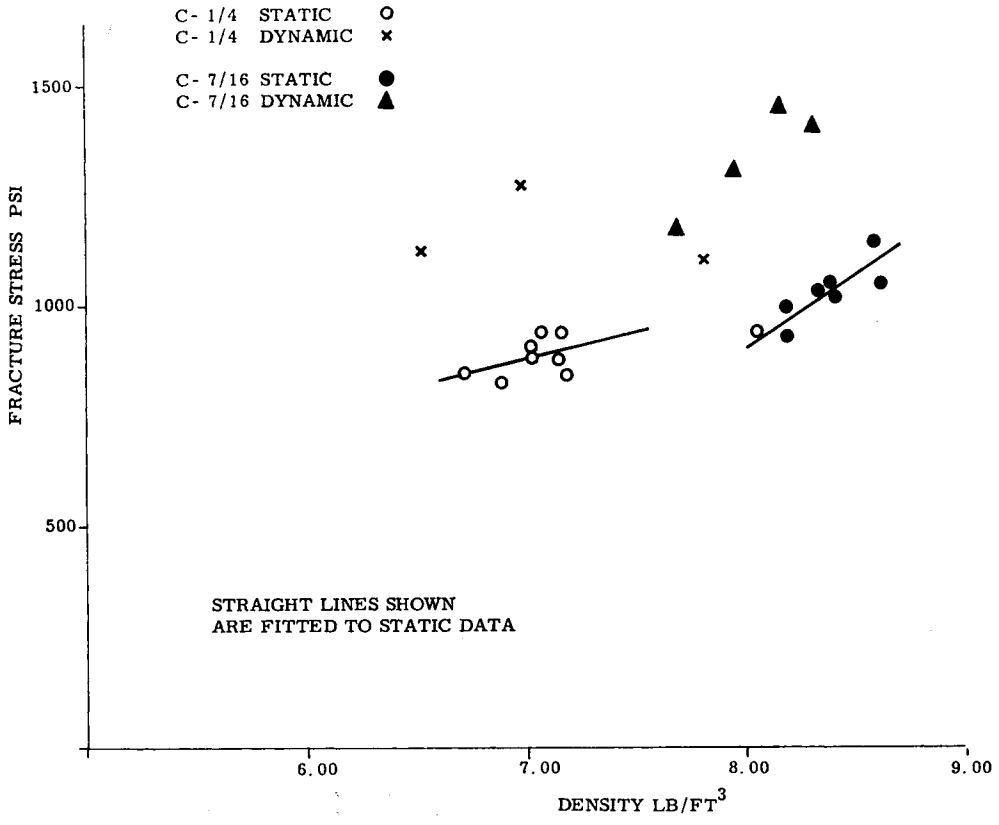

Fig. 12. Fracture stress versus density for cotton honeycomb.

the material absorbs less energy under the dynamic conditions than under static conditions. The amount of these differences attributable directly to strain-rate sensitivity cannot be determined with certainty from this investigation because of the difference in the manner in which the loads were applied. In the "static" test the load was applied at constant crosshead speed, whereas in the dynamic test the ram was initially at rest, then accelerated, and finally brought to rest again by the sample; the strain rate continuously varied from zero to maximum and back to zero.

To investigate the significance of the fracture strength data presented in Figures 10 through 12, the data were analyzed in the following manner. The best straight lines were calculated through each group of PVB, MDA, and 1100 points. Also, a best straight line was calculated through the combined points (Fig. 10). These fitted lines were statistically compared as shown in Table II.

TABLE II
Static Fracture Strength Correlation for Paper Honeycomb

	No. of data points	Fitted slope, psi/lb./ft.^{3}	Variability about fitted line, psi	95% confidence slope limits	Confidence level for significant difference from combined slope, %	Straight-line correlation coefficient
PVB	8	261	48.8	191–331	67	0.934
MDA	10	231	40.3	153–309	80	0.890
1100	10	314	87.4	229–400	65	0.924
Combined	28	288	90.8 •	253–323	—	0.936

In all cases the line fitting was done in the stress direction; i.e., the fracture stress was treated as a function of density. As shown in Table II, the line for the combined points exhibits the best correlation to a straight line and has the narrowest slope range at 95% confidence. Accordingly, the line plotted in Figure 10 is the best straight line through the data points of all the paper base samples. The corresponding dynamic data for the paper base samples (Fig. 11) were plotted in the same manner for comparison. In the case of the cotton base material (Fig. 12) there is better correlation of the lines through the individual groups of points, and these are presented.

Figures 10 and 11 provide the observation that the apparent density of paper-base honeycomb material of the same cell size seems to be a good measure of the strength level over the range of density and test conditions studied; however, the number of samples and the density range of each material were too limited to permit a definite conclusion to be drawn. It may also be observed that the resin system has a similar effect; e.g., PVB samples are generally stronger than MDA samples of the same density. Regardless of the cause of the overall strength-density correlation, its existence allows a comparison of the static and dynamic behavior of the paper honeycomb that is stronger over the entire density range than over three more limited density ranges. This strength–density correlation is of some independent interest when it is considered that the density variations of these samples had two different causes: the amount of resin applied in manufacture may vary from location to location in a large piece, and the method of cutting specimens from this large piece may include more or less of the dense double cell-wall areas in a particular sample.

A more detailed investigation would be necessary for an understanding of the mechanical basis of honeycomb strength, but the present simple observation, that increasing apparent sample density results in increasing strength, seems quite reasonable and could support the speculation that the strength of these honeycombs is derived from a structural interaction of the paper and resin and is not strongly influenced by variations in resin type or properties as long as this structural interaction remains unchanged.

The dependence of fracture strength on apparent density is also apparent for the cotton-base honeycomb materials (see Fig. 12). However, while the two groups of cotton-base samples were of the same material, they were of different cell sizes ($^1/_4$ in. and $^7/_{16}$ in.). Since fracture strength may be influenced by cell size as well as by density, a more detailed investigation would be necessary to fully evaluate the effect of each variable.

References

1. Joseph, J., *Materials & Methods*, **42**, No. 1, 98 (1955).
2. Stevens and Polentz, *Materials in Design Engineering*, **51**, No. 3, 117 (1960).
3. "Symposium on Honeycomb Structures," reprint *ASME*, 1960.
4. SAE Specification AMS 3720, AMS 3722.

Synopsis

Five organic crosslinked materials have been studied for compression properties at room temperature. Their static behavior (0.02 in./min.) and dynamic behavior (up to 1300 in./min.) have been measured as a function of the nature of the material or of its apparent density. The materials withstand a higher stress, 30 to 40%, and show a higher modulus of elasticity, about 100%, when subjected to rapid loading. Resistance to fracture is a linear function of the apparent density at two speeds. Equipment as well as methods are described.

Résumé

Les propriétés de compressibilité à température de chambre ont été étudiées dans le cas de cinq matériaux organiques réticulés. On a mesuré leurs comportements statique (0.02 pouce/minute) et dynamique (jusqu'à 1300 pouces/minute) en fonction de la nature du matériau et de sa densité apparente. Ces matériaux supportent une tension plus élevée de 30 à 40% et présentent un module de l'élasticité plus élevé d'environ 100%, lorsqu'ils sont soumis à une charge à vitesse élevée. La résistance à la rupture est une fonction linéaire de la densité apparente aux deux vitesses. On décrit l'équipement de même que les méthodes d'essais.

Zusammenfassung

Die Kompressionseigenschaften bei Raumtemperatur von fünf organischen Wabensystemen werden mitgeteilt. Statisches (0,02 inch/Minute) und dynamisches Verhalten (bis zu 1300 inch/Minute) wurden gemessen und werden als Funktion des Materials und der scheinbaren Dichte angegeben. Bei der höheren Geschwindigkeit konnten diese Materialien mit einer 30 bis 40 Prozent grösseren Spannung beansprucht werden und zeigten einen um ungefähr 100 Prozent höheren Elastizitätsmodul. Die Bruchfestigkeit erweist sich bei beiden Geschwindigkeiten als eine lineare Funktion der scheinbaren Dichte. Testapparat und -methoden werden beschrieben.